TiW(N) as Diffusion Barriers Between Cu and Si

Jung-Chao Chiou, Kuen-Chi Juang, and Mao-Chieh Chen*

Department of Electronics Engineering and the Institute of Electronics, National Chiao-Tung University, Hsinchu, Taiwan

ABSTRACT

TiW(N) and TiW are employed as diffusion barriers in the Cu/barrier/Si system. The thermal stability of Cu/TiW(N) and Cu/TiW contacted p^+n junction diodes was investigated with respect to metallurgical reaction and electrical characteristics. The as-deposited TiW film formed body-centered cubic (bcc) structure, while the TiW(N) film formed face-centered cubic (fcc) structure. The Cu/TiW(600 Å)/Si structure remains intact up to 750°C 30 s rapid thermal anneal (RTA) in N_2 ambient; at 775°C, the Cu diffuses through the TiW layer to form Cu_3Si with an overlayer of Ti-W-Si on the surface. The Cu/TiW(N)(600 Å)/Si system is metallurgically stable up to 1000°C 30 s RTA in N_2 ambient. The Cu/TiW(600 Å)/p^+n junction diodes were able to withstand the RTA annealing up to 675°C without losing the device integrity; however, the devices' characteristics are completely destroyed at temperatures above 775°C inconsistent with the occurrence of dramatic metallurgical reaction. The Cu/TiW(N)(600 Å)/p^+n junction diodes were able to withstand the RTA treatment up to 650°C without electrical characteristic degradation; and the devices' characteristics degrade gradually with the increase of RTA temperature.

Introduction

Copper has been considered as a potential metallization material in deep submicron integrated circuits because of its low resistivity (1.67 μΩ-cm for bulk) and superior high electromigration resistance.[1-5] However, copper acts as a deep-level contaminant in Si and reacts with Si to form the compound Cu_3Si at very low temperatures (200°C).[6-11] To use Cu as an interconnection metal, an effective diffusion barrier layer is required to protect underlying devices from Cu contamination.

Thermal stability of the Cu/diffusion-barrier/Si structure has been extensively studied lately to assess the potential of various diffusion barriers, and most of the results are summarized in Ref. 12. Among the various diffusion barrier materials, TiW [30:70 atom percent (a/o)] was found to be the most effective one.[12] TiW barrier has also been used in the Al/TiW/$CoSi_2$ and Cu/TiW/$CoSi_2$ systems and has proved to be a useful diffusion barrier layer.[13,14] In addition, it has been reported that incorporation of nitrogen and oxygen in TiW film can improve the barrier performance in Al(Cu-Si)/W-Ti(N)/SiO_2/Si and Au/TiW/Al/SiO_2/Si systems.[15-17] In this study, a TiW(N) layer, which was deposited by sputtering the $Ti_{0.3}W_{0.7}$ target in a mixing gas of Ar:N_2 = 1:5, was used as diffusion barrier in the Cu/TiW(N)/p^+n diode structure and its barrier effect metallurgically and electrically investigated.

* Electrochemical Society Active Member.

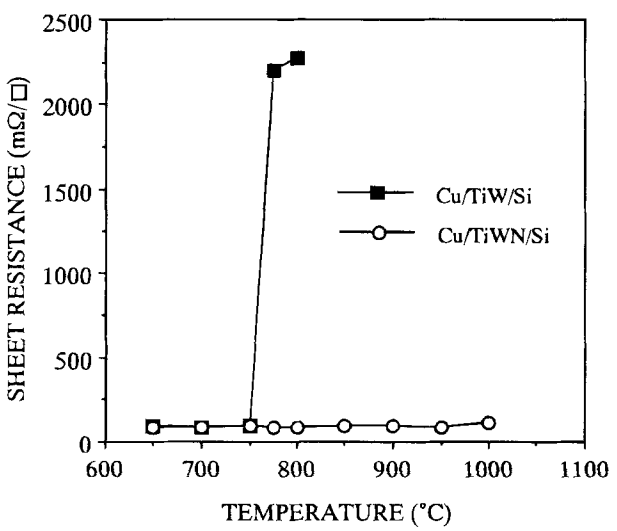

Fig. 1. Sheet resistance *vs.* annealing temperature for the Cu(2000 Å)/TiW(600 Å)/Si and Cu(2000 Å)/TiW(N)(600 Å)/Si samples.

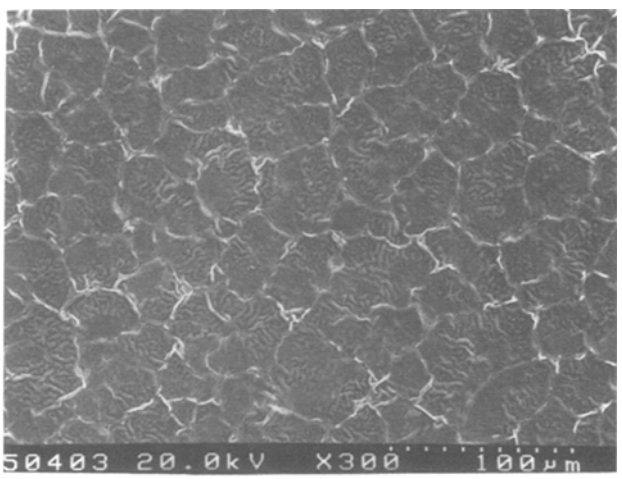

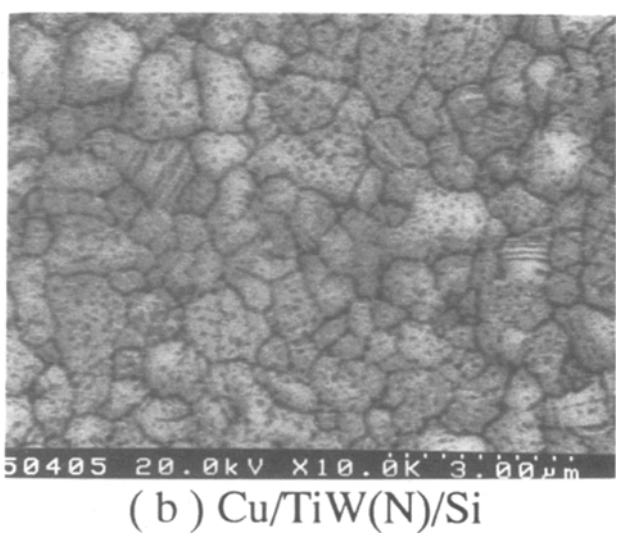

Fig. 2. SEM micrographs showing surface morphology for the (a) Cu(2000 Å)/TiW(600 Å)/Si and (b) Cu(2000 Å)/TiW(N)(600 Å)/Si samples after 900°C RTA in N_2 for 30 s.

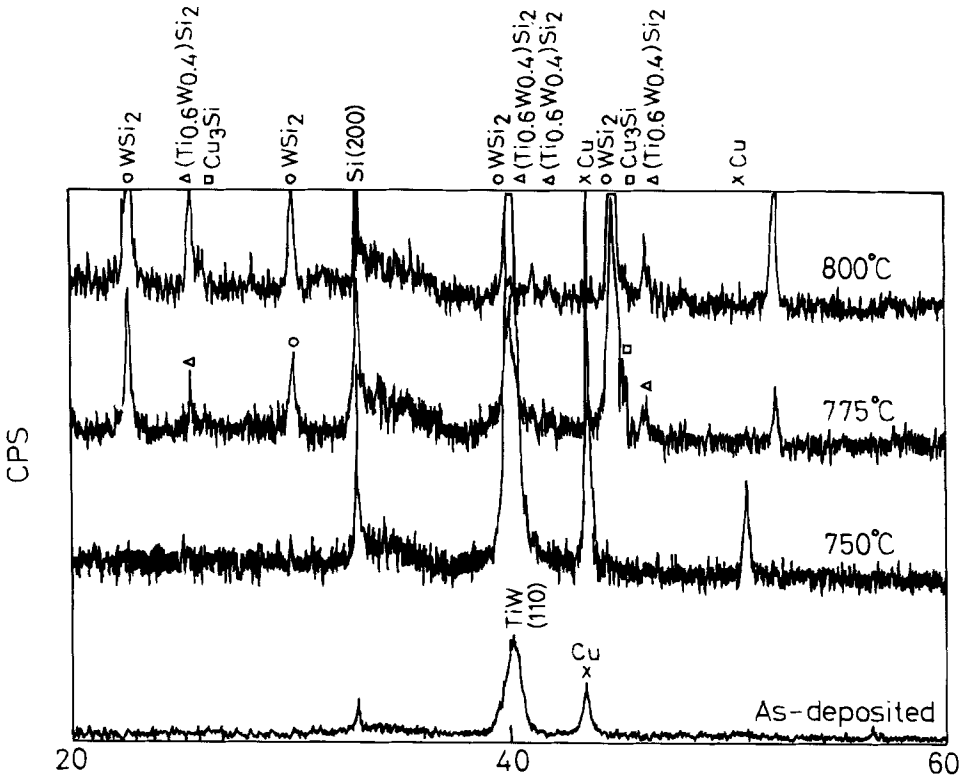

Fig. 3. The XRD spectra for the Cu(2000 Å)/TiW(600 Å)/Si sample: as-deposited and RTA annealed at 750, 775, and 800°C in N_2 for 30 s.

Experimental

Samples of Cu/TiW(N)/p⁺n and Cu/TiW/p⁺n diodes were fabricated for this study. The starting material was n-type, (100) oriented Si wafers with a nominal resistivity of 1 to 10 Ω-cm. After initial cleaning, a 6000 Å field SiO_2 was thermally grown in a pyrogenic steam atmosphere at 1050°C. Square contact regions with area of 2.5×10^{-3} cm^2 were defined by the photolithographic method. The samples were cleaned again and then oxidized to grow 250 Å screen oxide for ion implantation. The p⁺n junctions were formed by BF_2^+ implantation at 70 keV to a dose of 5×10^{15} cm^{-2} through the screen oxide, followed by annealing

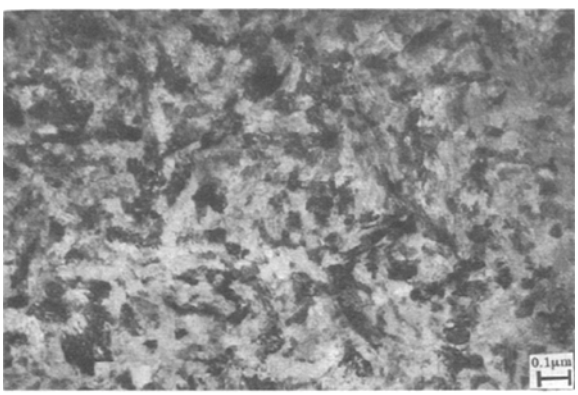

(a) Bright field plain view

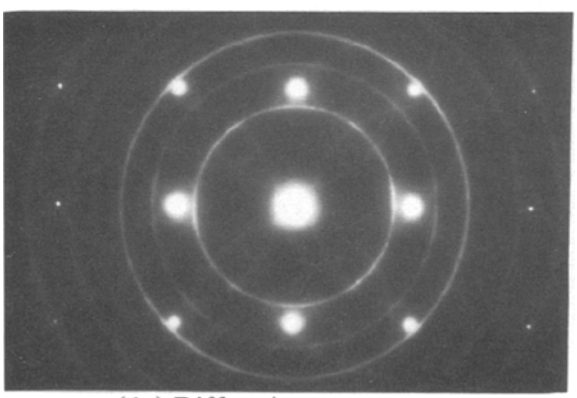

(b) Diffraction pattern

Fig. 4. EM micrographs of bright field plan view and diffraction pattern for the as-deposited TiW film: (a) plan view and (b) diffraction pattern.

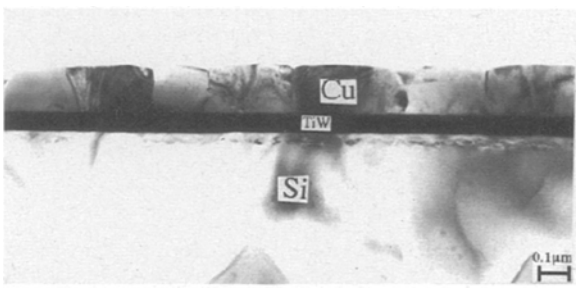

(a) 750°C

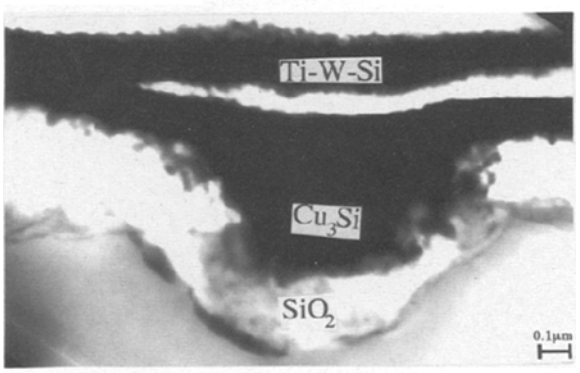

(b) 775°C

Fig. 5. TEM cross-sectional micrographs of the Cu(2000 Å)/TiW(600 Å)/Si sample after RTA annealing in N_2 for 30 s at (a) 750 and (b) 775°C.

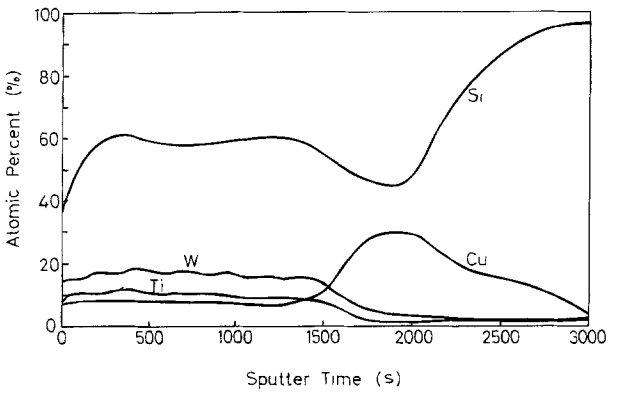

Fig. 6. Auger depth profile of the Cu(2000 Å)/TiW(600 Å)/Si sample after RTA annealing in N_2 for 30 s at 775°C.

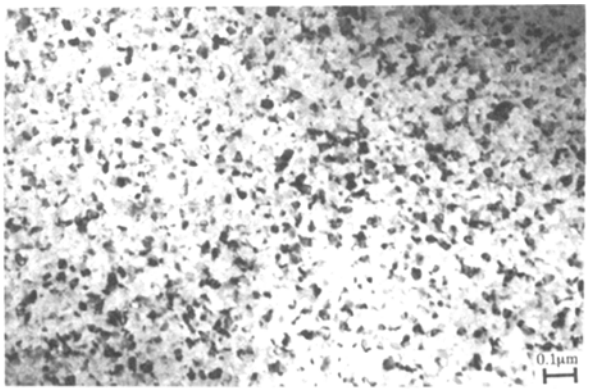

(a) Bright field plain view

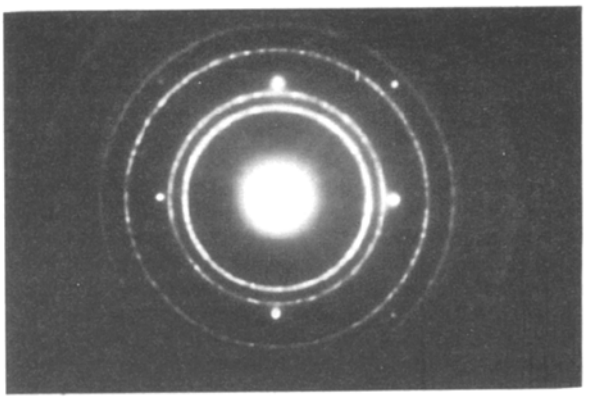

(b) Diffraction pattern

Fig. 8. TEM micrographs of bright field plan view and diffraction pattern for the as-deposited TiW(N) film: (a) plan view and (b) diffraction pattern.

at a temperature of 900°C for 90 min in N_2 ambient. A 600 Å thick TiW(N) or TiW barrier layer was deposited. The TiW(N) film was deposited by sputtering using the TiW [Ti:W 10:90 weight percent (w/o)] target in a gas mixture of Ar:N_2=1:5 ambient at a pressure of 5×10^{-3} Torr and with a deposition rate of 1.7 Å/s. The TiW layer was deposited using the same target and with the same conditions, except that pure Ar was used instead of an Ar/N_2 mixture. The samples were exposed to air and then the Cu deposition followed. An 1800 Å thick Cu film was deposited by sputtering a Cu target (99.99%) in Ar ambient at a pressure of 5×10^{-3} Torr; the deposition rate was 0.1 Å/s. The samples were patterned into individual diodes by wet etching, using an etching solution for the Cu film of 5% HNO_3, and a mixture of $NH_4OH + H_2O_2 + H_2O$ = 1:1:1 for the TiW(N) and TiW films. The completed samples were treated with rapid thermal annealing (RTA) for 30 s at temperatures ranging from 300 to 1000°C. Finally, Al metallization was applied to the back side of each wafer for electrical measurement. Unpatterned samples of Cu/TiW(N)/Si and Cu/TiW/Si structures were also fabricated following the same procedure for material analysis. Sheet resistance was measured by a four-point probe on the unpatterned samples. Surface morphology of the samples was inspected by scanning electron microscope (SEM). Scanning Auger microscope (SAM) was used for depth profile structure analysis. X-ray diffraction (XRD) spectroscopy was used for material phase identification. Transmission electron microscope (TEM) was used to study the interacted layer structures and for crystal structure identification. Electrical characteristics

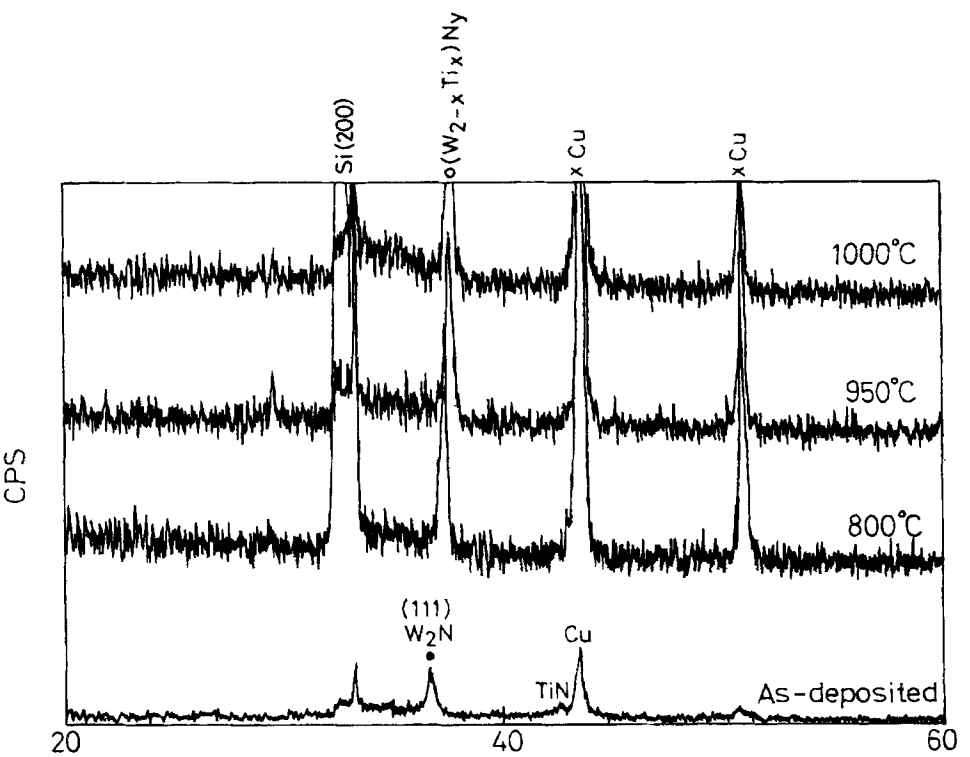

Fig. 7. The XRD spectra for the Cu(2000 Å)/TiW(N)(600 Å)/Si sample: as-deposited and RTA annealed at 800, 950, and 1000°C in N_2 for 30 s.

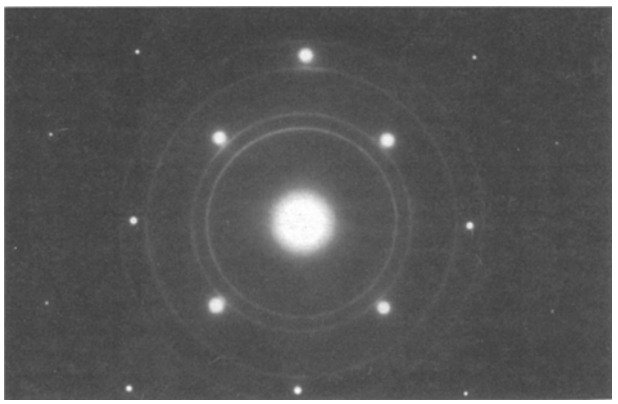

Fig. 9. TEM diffraction pattern for the TiW(N) film after RTA in N_2 for 30 s at 1000°C.

of the diodes were measured with a semiconductor parameter analyzer HP4145B.

Results and Discussion

Figure 1 shows the sheet resistance R_s of the Cu/TiW/Si and Cu/TiW(N)/Si samples after 30 s RTA at various temperatures. An abrupt R_s increase occurred on the Cu/TiW/Si sample after 775°C RTA; sample surface color also changed from reddish yellow to silver-gray, suggesting that some metallurgical reaction had occurred. On the other hand, only a small R_s variation was observed on the Cu/TiW(N)/Si sample. In addition, the sample surface remained reddish yellow Cu color even after reaching 1000°C RTA, although it became slightly less glossy looking.

Surface morphology of the Cu/TiW/Si and Cu/TiW(N)/Si samples after RTA at 900°C is illustrated in Fig. 2. The Cu/TiW/Si sample (Fig. 2a) looks silver-gray, appears to be made up of grains (identified as W-Ti-Si as explained later in this section) about 30 μm in size, and has a rough surface morphology. Surface morphology of the Cu/TiW(N)/Si sample (Fig. 2b) shows that it is composed of compact Cu grains about 1.5 μm in size.

The XRD results from the Cu/TiW/Si sample illustrated in Fig. 3 show that Cu and TiW reacted with Si to form compounds of WSi_2, $(Ti_{0.6}W_{0.4})Si_2$, and Cu_3Si after 30 s RTA at 775°C. The XRD (110) peak of the TiW film indicates that the lattice constant of the TiW film is 3.177 Å. TEM techniques were used to make a more detailed study of the TiW film. Figure 4 illustrates the bright field plan view micrograph and the diffraction pattern of the as-deposited TiW film, which is composed of intersected grains about 1000 Å in size. The diffraction pattern shows that the crystal structure of the TiW film is body-centered cubic (bcc) with a lattice constant of 3.178 Å, results consistent with the XRD analysis. TEM analysis of the 750°C annealed TiW film (not shown) revealed that the film's crystal and grain structures were almost identical with those of the as-deposited TiW film. The TEM cross-sectional micrographs of the Cu/TiW/Si sample shown in Fig. 5 reveal that the Cu/TiW/Si structure remained intact after RTA at 750°C (Fig. 5a). After RTA at 775°C, the structure was completely destroyed by the formation of silicides; the TEM cross-sectional views show a Cu_3Si precipitate surrounded by SiO_2 intruding into the Si substrate, as well as a compound layer covering the top surface. The Auger depth profile of the Cu/TiW/Si sample after RTA at 775°C shown in Fig. 6, indicates that Cu has diffused toward the Si substrate and formed Cu-silicide, while the surface layer is mainly a compound layer of Ti-W-Si. From the XRD, Auger depth profile, and TEM results, we can conclude that a dramatic metallurgical reaction occurred within the Cu/TiW/Si structure at a temperature of 775°C. Copper first diffused across the TiW layer and formed Cu_3Si phase at some weaker points; then, the TiW layer was transformed into the compound Ti-W-Si on the surface, which exhibited a rough grain structure silver-gray in color as illustrated in Fig. 2a.

The XRD results from the Cu/TiW(N)/Si sample are illustrated in Fig. 7. It was found that the as-deposited TiW(N) film contained a mixture of W_2N and TiN phases. The corresponding bright field TEM plan view and diffraction

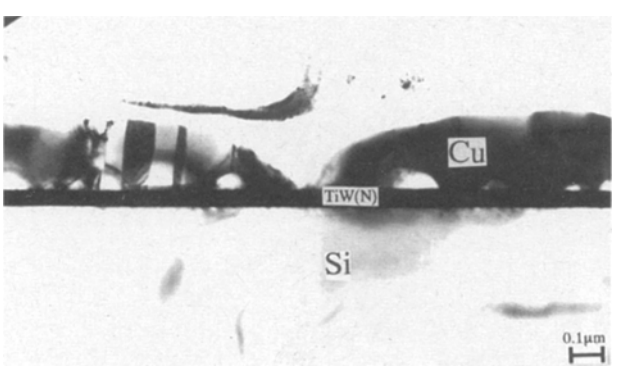

Fig. 10. Cross-sectional view TEM micrograph for the Cu(2000 Å)/TiW(N)(600 Å)/Si sample after RTA annealing in N_2 for 30 s at 1000°C.

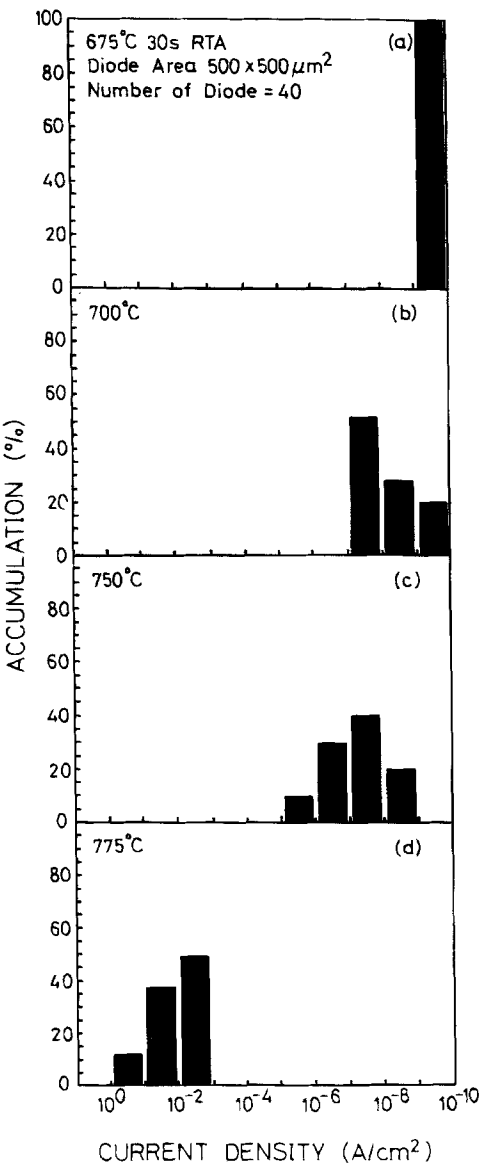

Fig. 11. Histogram of the reverse leakage current density for the Cu(2000 Å)/TiW(600 Å)/p⁺n diodes annealed with RTA at (a) 675, (b) 700, (c) 750, and (d) 775°C. All leakage currents were measured at −5 V bias.

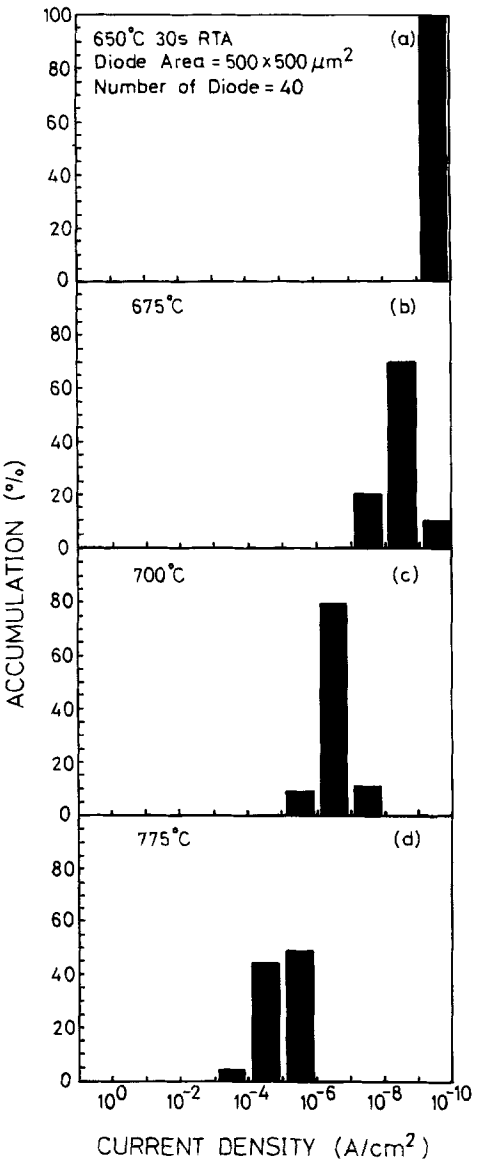

Fig. 12. Histogram of the reverse leakage current density for the Cu(2000 Å)/TiW(N)(600 Å)/p⁺n diodes annealed with RTA at (a) 650, (b) 675, (c) 700, and (d) 775°C. All leakage currents were measured at −5 V bias.

pattern of the as-deposited TiW(N) film in Fig. 8 show the as-deposited TiW(N) film to be composed of compact grains about 100 Å in size, and the diffraction pattern reveals that the as-deposited film has a face-centered cubic (fcc) structure. Furthermore, the diffraction pattern seems to be composed of two closely spaced fcc diffraction rings. Both the W_2N (ASTM Card:251257) and the TiN (ASTM Card:381420) phases have fcc structures with lattice constants of 4.126 Å (W_2N) and 4.241 Å (TiN), respectively, while the lattice constant estimated from the average radius of the diffraction ring for the as-deposited TiW(N) film is 4.208 Å, which is close to the lattice constants of W_2N and TiN. The XRD spectra in Fig. 7 also show that the W_2N phase remained stable, and no metallurgical reaction was observed on the Cu/TiW(N)/Si structure up to 1000°C. In addition, the shift of the W_2N (111) peak indicates that the lattice constant decreased after RTA. The TEM plan view of the 1000°C RTA annealed TiW(N) film (not shown) revealed that the annealed film had a grain structure identical to that of the as-deposited film. The diffraction pattern of the 1000°C RTA annealed TiW(N) film as shown in Fig. 9 indicates that the annealed film had a single-phase fcc structure with a lattice constant of 4.178 Å, which is smaller than that of the as-deposited TiW(N) film (4.208 Å). From the consistency of the XRD and TEM analysis results, we can conclude that the as-deposited TiW(N) film consists of major W_2N and minor TiN phases, and no obvious metallurgical reaction occurred in the Cu/TiW(N)/Si structure up to 1000°C during RTA. Nevertheless, after the RTA annealing, the TiN phase vanished, and the lattice constant of TiW(N) decreased. Since the atomic radius of Ti (1.475 Å) is close to that of W (1.37 Å) and is much smaller than that of N (2.83 Å), it is possible that, after high temperature annealing, Ti and N atoms in the TiN dissolved into the W_2N structure forming the $(Ti_xW_{2-x})N_y$ compound and thus inducing the lattice constant shift.

Figure 10 shows the TEM cross-sectional micrograph of the 1000°C annealed Cu/TiW(N)/Si sample. The structure was basically preserved after 30 s RTA at 1000°C; however, some voids were formed between Cu and the TiW(N) layers, and the Cu film had obviously undergone a reflow process which created a rough surface. The roughness and porosity of the Cu film supposedly resulted in a slight increase of R_s and a fuzzy looking sample surface.

Figure 11 shows the distribution of reverse leakage current density J_r measured at −5 V on 40 randomly chosen Cu/TiW/p⁺n junction diodes. The diode characteristics degraded after RTA at 700°C, and further deteriorated with further increases in annealing temperature. After 775°C annealing, all junctions were severely damaged (Fig. 11d), which is consistent with the dramatic metallurgical reaction that occurred at this temperature. Similar J_r measurements were made on the Cu/TiW(N)/p⁺n junction diodes, and the results are illustrated in Fig. 12. Although the Cu/TiW(N)/Si structure is more metallurgically stable than the Cu/TiW/Si structure, the Cu/TiW(N)/p⁺n diodes started to degrade at a slightly lower annealing temperature of 675°C, and the junction degraded gradually as annealing temperature was increased. Figure 13 shows the average leakage current density *vs.* annealing temperature for the Cu/TiW/p⁺n and Cu/TiW(N)/p⁺n junction diodes. The Cu/TiW(N)/p⁺n diodes apparently become more stable electrically than the Cu/TiW/p⁺n diodes when the annealing temperature exceeds 775°C. Degradation of the Cu/barrier/Si junction structure, electrical characteristics always occurs before the metallurgical reaction. Since Cu is a fast diffusion species in Si, degradation of the junction will depend on whether the barrier layer can or cannot prevent the Cu from penetrating through the barrier layer. Although the Cu/TiW(N)/Si system is more metallurgically stable than the Cu/TiW/Si system, and we did hope that the incorporated nitrogen would be segregated at the grain boundaries to retard the diffusion paths for Cu atoms, the diffusion-barrier effect of TiW(N) apparently did not prevent Cu penetration. It is possible that the smaller grains in the TiW(N) layer offer more path alternatives for Cu diffusion.

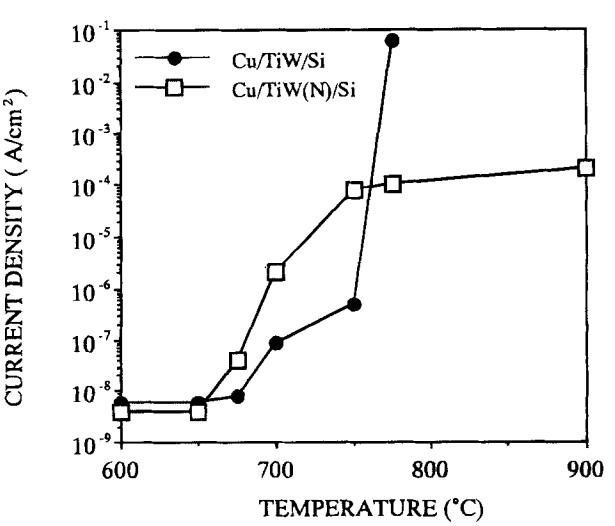

Fig. 13. Average reverse leakage current density measured at −5 V for the RTA annealed Cu(2000 Å)/TiW(600 Å)/p⁺n and Cu(2000 Å)/TiW(N)(600 Å)/p⁺n junction diode.

Conclusion

Thermal stability of Cu/TiW(600 Å)/p^+n and Cu/TiW(N) (600 Å)/p^+n diodes were investigated with respect to the diffusion-barrier effects of TiW and TiW(N) barrier layers for Cu metallization. The TiW film has a W bcc structure, while the TiW(N) film has a W_2N fcc structure. The Cu/TiW/Si system is metallurgically stable up to 30 s RTA annealing at 750°C, while the Cu/TiW(N)/Si structure remains basically stable up to 1000°C. The Cu/TiW/Si structure was destroyed after RTA annealing at 775°C with the formation of a Cu_3Si phase that intruded into the Si substrate, and the formation of a W-Ti-Si compound layer covering the sample surface. The electrical characteristics of the Cu/TiW/p^+n junction diodes started to degrade at 700°C, and the diodes' reverse current made a drastic increase at 775°C. On the other hand, the Cu/TiW(N)/p^+n junction diodes started to degrade at 675°C, and the reverse current increased gradually with increasing annealing temperature. As a result, the J_r of the Cu/TiW(N)/p^+n diodes is smaller than that of the Cu/TiW/p^+n diodes after RTA annealing at temperatures above 775°C.

Acknowledgment

The authors wish to thank the Semiconductor Research Center of National Chiao-Tung University and the National Nano Device Laboratory for providing excellent processing environment. This work was supported by the National Science Council, ROC, under Contract No. NSC-82-0404-E009-400.

Manuscript submitted Sept. 12, 1994; revised manuscript received Jan. 17, 1995.

National Chiao-Tung University assisted in meeting the publication costs of this article.

REFERENCES

1. H. K. Kang, J. S. H. Cho, and S. S. Wang, *IEEE Electron Device Lett.*, **EDL-13,** 448 (1992).
2. C. W. Park and R. W. Vook, *Appl. Phys. Lett.*, **59,** 175 (1991).
3. J. Tao, N. W. Cheung, C. Hu, H. K. Kang, and S. S. Wang, *IEEE Electron Device Lett.*, **EDL-13,** 433 (1992).
4. P. L. Pai, C. H. Ting, C. Chiang, C. S. Wei, and D. B. Fraser, *Mater. Res. Soc. Symp. Proc. VLSI V,* p. 359 (1990).
5. T. E. Seidel, *Mater. Res. Soc. Symp. Proc.*, **260,** 3 (1992).
6. A. Cros, M. O. Aboelfotoh, and K. N. Tu, *J. Appl. Phys.*, **67,** 3328 (1990).
7. S. H. Corn, J. L. Falconer, and A. W. Czanderna, *J. Vac. Sci. Technol.*, **A6,** 1012 (1988).
8. S. Q. Hong, C. M. Comrie, S. W. Russell, and J. W. Mayer, *J. Appl. Phys.*, **70,** 3655 (1992).
9. R. Padiyath, J. Seth, S. V. Babu, and L. J. Matienzo, *ibid.*, **73,** 2326 (1993).
10. L. Stolt, F. M. D'Huerle, and J. M. E. Harper, *Thin Solid Films,* **200,** 147 (1991).
11. S. D. Brotherton, J. R. Ayres, A. Gill, H.W. van Kesteren, and F. J. A. M. Greidanus, *J. Appl. Phys.*, **62,** 1826 (1987).
12. S. Q. Wang, S. Suthar, C. Hoeflich, and B. J. Burrow, *ibid.*, **73,** 2301 (1993).
13. F. M. Yang and M. C. Chen, *J. Vac. Sci. Technol.*, **B11,** 744 (1993).
14. J. C. Chiou and M. C. Chen, *This Journal,* **141,** 2804 (1994).
15. J. M. Oparowski, R. D. Sisson, Jr., and R. R. Biederman, *Thin Solid Films,* **153,** 313 (1987).
16. A. G. Dirks, R. A. M. Wolters, and A. J. M. Nellissen, *ibid.*, **193/194,** 201 (1990).
17. R. S. Nowicki, J. M. Harris, M. A. Nicolet, and I. V. Mitchell, *ibid.*, **53,** 195 (1978).